GANIL

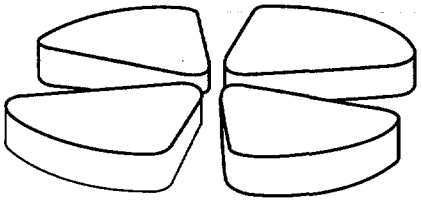

Phase Transition in Finite Systems

Philippe CHOMAZ[1], Veronique DUFLOT[1,2] and Francesca GULMINELLI[2]
[1]G.A.N.I.L.(CEA-DSM/IN2P3-CNRS), BP 5027, 14076 CAEN cedex 5, FRANCE.
[2]LPC Caen, (IN2P3-CNRS/ISMRA et Universite), F-14050 Caen cedex, France

Invited Plenary Talk to the
Bologna International Conference, Bologna 2000

GANIL P 00 39

Phase Transition in Finite Systems

Philippe CHOMAZ[(1)], Veronique DUFLOT[(1,2)] and Francesca GULMINELLI[(2)]
[(1)]G.A.N.I.L.(CEA-DSM/IN2P3-CNRS), BP 5027, 14076 CAEN cedex 5, FRANCE.
[(2)]LPC Caen, (IN2P3-CNRS/ISMRA et Universite), F-14050 Caen cedex, France

In this paper we present a review of selected aspects of Phase transitions in finite systems applied in particular to the liquid-gas phase transition in nuclei. We show that the problem of the non existence of boundary conditions can be solved by introducing a statistical ensemble with an averaged constrained volum. In such an ensemble the microcanonical heat capacity becomes negative in the transition region. We show that the caloric curve explicitely depends on the considered transformation of the volume with the excitation energy and so does not bear direct informations on the characteristics of the phase transition. Conversely, partial energy fluctuations are demonstrated to be a direct measure of the equation of state. Since the heat capacity has a negative branch in the phase transition region, the presence of abnormally large kinetic energy fluctuations is a signal of the liquid gas phase transition.

1. INTRODUCTION

Since nuclear forces resemble to Van der Waals interactions the nuclear phase diagram is expected to present a liquid gas phase transition (see figure 1). Our present knowledge of the nuclear equation of state is limited. The main reason is the difficulty to treat the nuclear many-body problem and to define a reliable in medium interaction. The saturation energy and density, i.e. the ground state of nuclear matter, are well established but the compressibility, i.e. the variation of the energy as a function of the density around the saturation point, is still under discussion because of the recent results of relativistic approaches. As far as the temperature dependence of nuclear properties is concerned very little is also know in an absolute way. Only the entropy variation, i.e. the level density parameter $a = S/T$, of a finite nucleus as an open system has been clearly established through evaporation studies. A huge research activity is now devoted to the extraction of reliable information of the nuclear equation of states and the associated phase diagram. Heavy ion reactions are routinely used to test mechanical and thermodynamical properties of nuclei. In the recent years the multifragmentation regime has been tentatively associated with the occurrence of a liquid-gas phase transition. The main problem is to link the dynamics of a collision with the extraction of meaningful thermodynamical quantities. It is rather surprising that a huge amount of experimental data can be explained by many different models. For example figure 2 shows that the experimental data obtained in the Xe+Sn reaction at 32 MeV/nucleon can be explained by a dynamical simulation of the phase transition as well as by a simple statistical model. This may indicate that the dynamics is sufficiently chaotic to populate the whole phase space. As a concequence

a thermodynamical approach might be justified. In the following we will concentrate on the properties of a nuclear system in a statistical equilibrium.

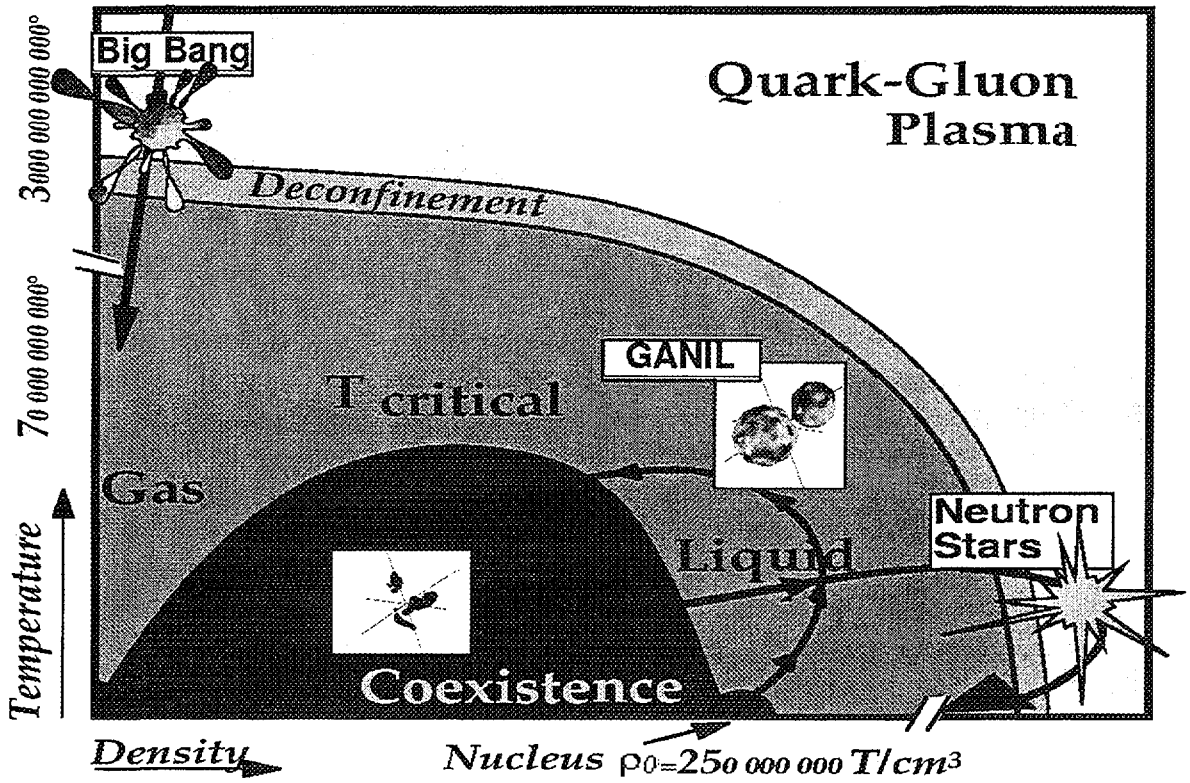

Figure 1. Nuclear Phase diagram in the temperature density plane. At low temperature and below the saturation density ρ_0 a liquid gas phase transition is expected. In extrem conditions the matter should become a plasma of free quarks and gluons. Three cosmic events are also schematically drawn the Big-Bang, the collapse of a supernova toward a neutron star and a heavy ion collision at GANIL.

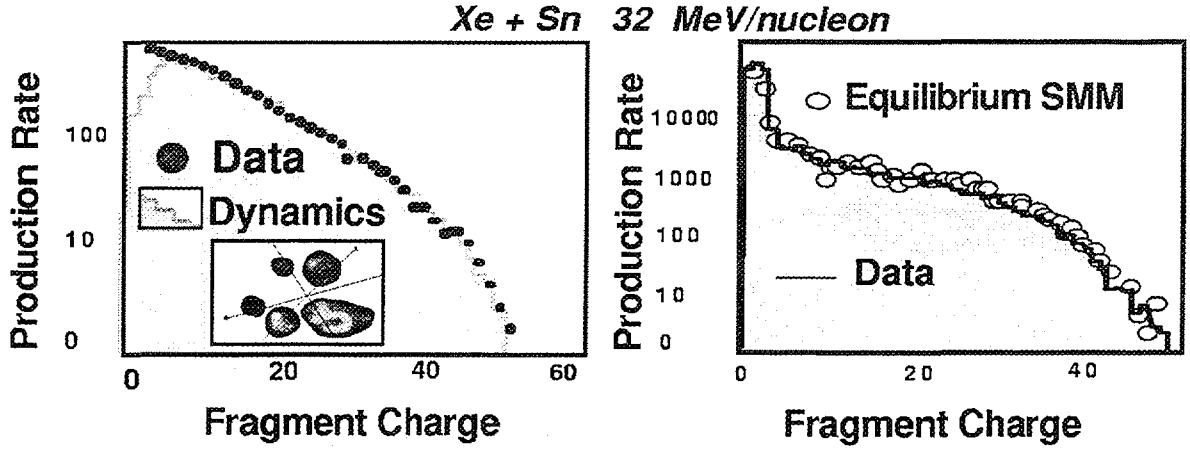

Figure 2. Experimental data from the INDRA collaboration on Xe+Sn at 32 MeV/nucleon compared with a dynamical simulation (left) and a statistical approach (right) (from ref. [1]).

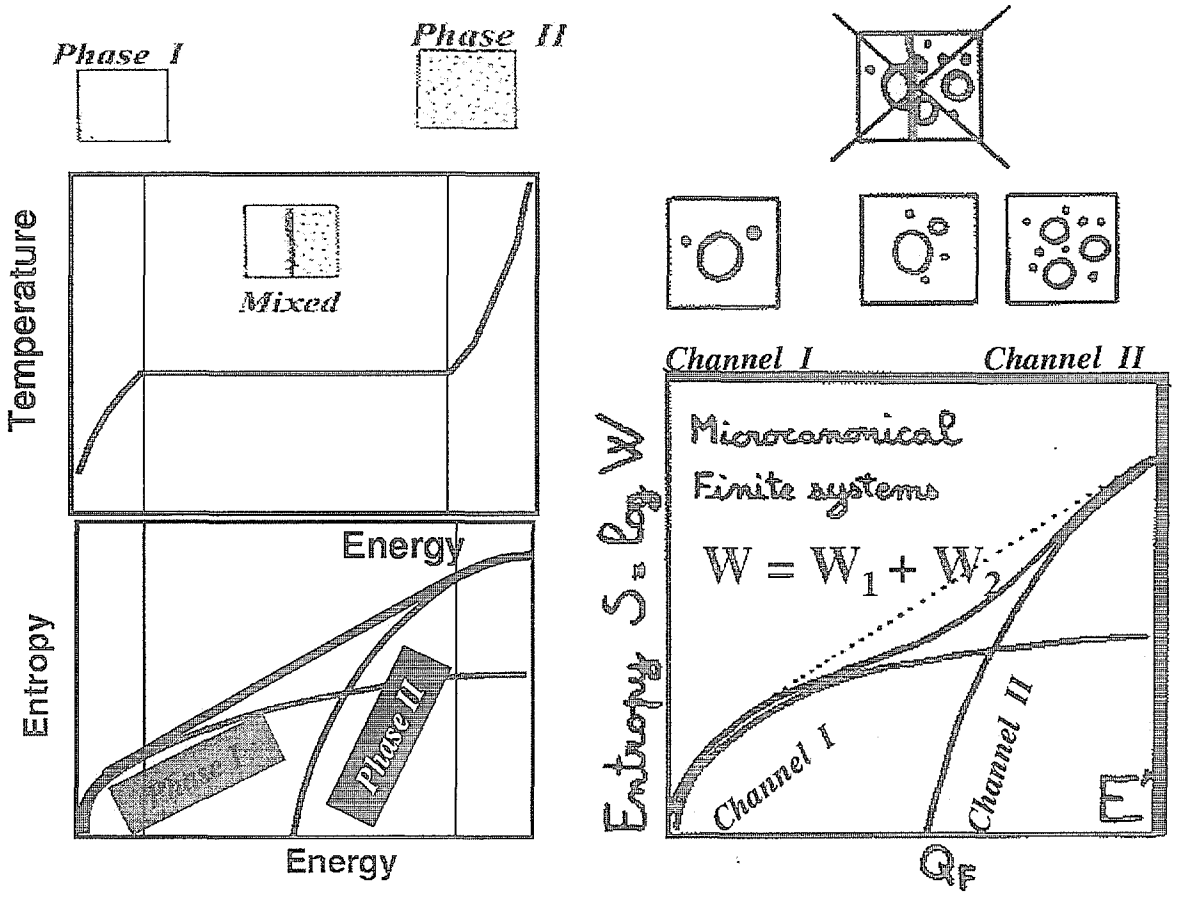

Figure 3. On the left the typical evolution of the entropy and the associated temperature of an infinite system undergoing a phase transition. The linear entropy region corresponds to the constant temperature characteristic of a phase transition. On the right the typical evolution of a finite system. Schematic pictures of the system at the phase transition are also shown. (see text)

2. FROM INFINITE TO FINITE SYSTEMS

2.1. Phase transition in infinite systems

Phase transition are routinely encountered in the everyday life. Everybody knows that a boiling water keeps a constant temperature during the whole boiling process (since the pressure is usually constant). It should be noticed that this "kitchen"-experiment is in fact a microcanonical type of thermodynamics since we usually control the amount of energy (the fire) given to the system (the water in the kettle). This amazing constancy of the temperature can easily be understood at the thermodynamical limit. Indeed, at this limit the state of the system is the one which maximizes the entropy because the fluctuations around this maximum are neglected. Moreover, if we split the system in two parts containing a fraction λ and $(1-\lambda)$ respectively of the total mass of the system, again because we assume that in the thermodynamical limit we can neglect the role of

interfaces on both energy and entropy we can construct a macro-state giving the energy $e_1 = \lambda E_1$ to the first part and $e_2 = (1-\lambda) E_2$ to the second part. The total energy and entropy of this mixed events is simply

$$E = e_1 + e_2 = \lambda E_1 + (1-\lambda) E_2 \quad (1)$$
$$S = s_1 + s_2 = \lambda S_1 + (1-\lambda) S_2 \quad (2)$$

Indeed, the number of mixed states is simply the number of states in the first part $W_1 = \exp s_1 = \exp \lambda S_1$ times the number of states in the second part $W_2 = \exp s_2 = \exp (1-\lambda) S_2$.

If in some region the introduction of such mixed events leads to an entropy which is greater that the original one the mixed event will be infinitely more probable that the original one. If fact any mixing which maximized the entropy will win. Since S and E are in the mixed region simple linear functions of the mixing proportion λ the entropy is a straight line so that its derivative, the microcanonical temperature, remains constant. This is nothing but the Maxwell construction. This is the reason why at the thermodynamical limit the entropy should always be concave. This thermodynamical scenario is shown in the left part of figure 3.

2.2. Channel opening in finite systems.

In a finite system the simple argument about the mixed events does not hold anymore. Indeed, gluing two parts in proportion λ and $(1-\lambda)$ of two classes of events associated with the energy E_1 and E_2 does not generate a class of events at energy $E = \lambda E_1 + (1-\lambda) E_2$ because we cannot neglect the energy cost paid in terms of interfaces. Therefore neither the energy nor the entropy are expected to be additive and mixed events may not be the most important one. In fact, in finite systems the thermodynamics cannot be reduced to the most probable but rather the fluctuations are expected to be an essential phenomenon in finite systems. The Maxwell construction is therefore not possible any more and the construction of mixed event is not the way we may think about a phase transition. Nothing then prevents the entropy to present concave regions. It has been proposed that a concave anomaly can be considered as a general definition of phase transitions in finite systems[2,3]. This idea has been generalized to any convexity anomaly of any generalized thermodynamical potential[4].

If mixing is no more possible, sorting in categories remains a way to understand the transition from one type of event to another. In general many different types of events have to be considered in a phase transition region. In the infinite system one may think to classify events according to their proportion λ of one of the two phases, in finite systems fewer categories can be defined. For simplicity let us introduce only two types (labelled 1 and 2) of events on the basis of a large difference in an observable which can be thought as the order parameter. These two categories can be thought as two different channels. Far from the transition region only one of the two channels dominates. This can be the case if we have not yet passed the energy threshold for the opening of the second channel. As soon as we pass this threshold the competition or the relative probability of the two channels will be fixed by the respective degeneracies $W_1 = \exp S_1$ and $W_2 = \exp S_2$. Since we are only sorting events en categories the total degeneracy of the considered energy is

simply

$$W = W_1 + W_2 \tag{3}$$

If the entropy increase of the second channel is fast then it may rapidly overcome the first one leading to a concave anomaly in the total entropy $S = \log W$. This demonstrates that the idea of channel opening is intimately linked to the idea of phase transition.

3. MODELS FOR PHASE TRANSITION IN FINITE SYSTEMS.

3.1. Lattice-gas model

Let us first test these ideas on an exactly solvable model for second and first order phase transitions, the Lattice Gas Model of Lee and Yang [5]. This is a simplified model which can be interpreted as a schematic representation of a classical fluid with a Van der Waals type of equation of state. In our numerical implementation the N sites of a lattice are characterized by an occupation number $\tau = 0$ or 1 (see figure 3). Particles occupying nearest neighboring sites interact with an energy ϵ. A kinetic energy term is also included so that the Hamiltonian is given by

$$\hat{\mathbf{H}} = \sum_{i=1}^{N} \frac{p_i^2}{2m}\tau_i + \sum_{i,j}^{N} \frac{\epsilon}{2}\tau_i\tau_j \tag{4}$$

where the second sum runs only over neighboring sites.

In the liquid-gas phase transition, since the order parameter is the density difference between the two phases, the volume is essential in determining thermodynamical properties. Many studies have been performed considering periodic boundary conditions in order to avoid the effects of the surface [4,6,7]. Systems in a fixed cubic volume have also been investigated [8,9]. In the experimental case however the volume is not defined through boundary conditions because we are dealing with an open system. However, a typical average size of the fragmenting system might be deduced from experimental observables. For example the (average) radius of a hot source can be defined through interferometry or through comparisons with statistical models. From a theoretical point of view this implies that at equilibrium the entropy of the system should be maximized under the constraint of a specific value for the average volume. In the absence of a preferred direction, an average volume can be defined through the one-body observable [10,11]

$$\hat{\mathbf{V}} = \frac{4\pi}{3N} \sum_{i=1}^{N} r_i^3 \tau_i \tag{5}$$

where r_i is the distance to the center of the lattice.

Introducing first a canonical description in which the energy observable $\hat{\mathbf{H}}$ as well as the volume $\hat{\mathbf{V}}$ are known in average we have to introduce the associated Lagrange multipliers β, λ so that the partition function reads

$$Z_{\beta,\lambda} = \sum_{(n)} \exp\left(-\beta U^{(n)} - \lambda V^{(n)}\right) \tag{6}$$

Here, $U^{(n)}$ and $V^{(n)}$ are the expectation values of the operators $\hat{\mathbf{H}}$ and $\hat{\mathbf{V}}$ in the n^{th} event, β is the inverse of the canonical temperature $\beta = 1/T_{can}$, and the quantity $P = -\lambda/\beta$

has the dimension of a pressure. In other words, the experimental fact that the volume is known only in average means that the pressure, interpreted as the Lagrange multiplier associated with the volume observable, can be considered as the relevant state variable. A statistical ensemble of events associated with an average volume can easily be generated through a canonical sampling using a constrained Hamiltonian $\hat{\mathbf{E}}= \hat{\mathbf{H}}-P\ \hat{\mathbf{V}}$ where $P\ \hat{\mathbf{V}}$ can be considered as a constraining one-body external field. The averaged constrained energy $E = U - PV$ can be interpreted as an enthalpy. The actual value of the pressure parameter must be defined to get the desired average volume.

For finite systems the various ensembles are not equivalent because fluctuations cannot be neglected. Since energy is a directly accessible observable in each event, the correct statistical framework is the microcanonical ensemble. An easy way to access microcanonical quantities is to sort the canonical partitions according to their total energy. It is important to notice that this procedure may be in some cases numerically time consuming but it is an exact method to generate constant energy events with the correct microcanonical weight (see eq.(7) below). When both energy and volume are considered as thermodynamical observables one should in principle sort the canonical events sampled for a given temperature and pressure as a function of the energy and the volume. However, if the pressure is fixed it is sufficient to sort the events as a function of the constrained energy E. At a given temperature β the canonical distribution reads

$$P_\beta(E) = \frac{W(E)}{Z_\beta} \exp(-\beta E) \tag{7}$$

where W is the degeneracy of the state. In a sampling of N_0 events the probability P_β can be estimated from the number N_β of events falling in the enthalpy bin of size ΔE around E, $P_\beta(E)\,\Delta E \approx N_\beta(E)/N_0$. The bin size ΔE is chosen small enough that the results are independent of ΔE. Equation (7) can be inverted leading to the entropy $S(E) \equiv \log(W(E))$. This allows a direct estimation of the microcanonical caloric curve

$$T^{-1}(E) \equiv \frac{\partial S(E)}{\partial E} = \beta + \frac{\partial \log N_\beta(E)}{\partial E} \tag{8}$$

which is valid for every β. With a single microcanonical sampling at an arbitrary β it is in principle possible to directly compute the whole microcanonical caloric curve (8) without any approximation. However for a given β the energies far away from the canonical average $\bar{E}(\beta)$ are hardly sampled in the canonical ensemble. To minimize numerical inaccuracies it is therefore more convenient to perform many canonical samplings at different β and get T as the weighted average of the different estimations.

In the calculations shown below a number $A = 216$ of particles is fixed; to illustrate a first order phase transition the pressure P is chosen in such a way that the isobar crosses the canonical coexistence line at about the half of the critical temperature. The numerical realization of the model is a three dimensional cubic lattice characterized by a size large enough ($N = 8000$) so that the boundary conditions do not affect the calculations with a constraining pressure. Canonical statistical averages are taken over events obtained with a standard Metropolis sampling of the lattice occupations according to the partition function (6). The qualitative results of our analysis are not modified by varying the size of the system; however the actual values of the temperature and heat capacity do depend on

A due to finite size and, more important, surface effects. This implies that for a practical application to fragmentation data it is essential to study a constant mass source over the whole excitation energy range.

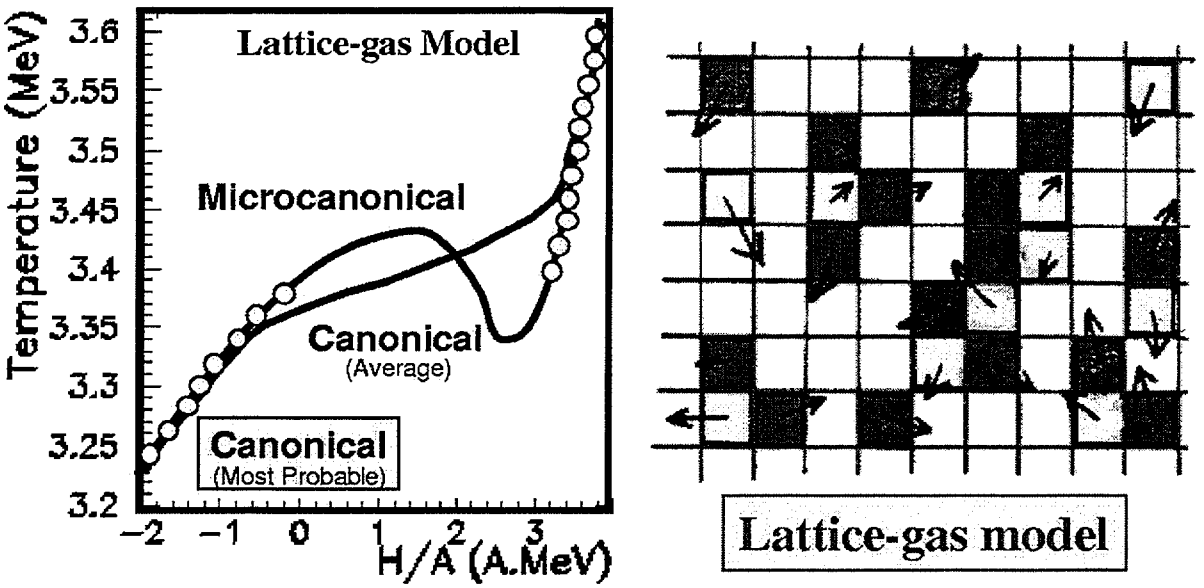

Figure 4. Right schematic drawing of the lattice-gas model. Left : Microcanonical caloric curve (full line) compared with the most probable (dots) and average (line) canonical energy for each β.

It is interesting to compare the microcanonical and canonical caloric curves as shown in Figure 4. In finite systems two canonical caloric curves can be defined, corresponding to the average and most probable energy associated to a given β. In infinite systems these two energies are equal because fluctuations can be neglected. Far from the phase transition the canonical and microcanonical curves agree. Indeed, from equation (8) we can see that the most probable canonical energy is characterized by the equality of the microcanonical and canonical temperatures. In the coexistence region however the predictions of the two ensembles differ in an noticeable manner. The canonical caloric curves are by definition monovaluated while this restriction does not apply to the microcanonical case. The microcanonical caloric curve presents a back bending while in the back-bending region the canonical caloric curve associated with the most probable energy presents a discontinuity equivalent to the Maxwell construction. The observed energy jump is directly related to the latent heat of the first order phase transition. Because of fluctuations the average energy presents a smoother behavior with however a clear slope change in the transition region. Allowing a fluctuating volume is essential to obtain the caloric curves of Figure 4: constant volume lattice gas calculations produce smoothly increasing caloric curves [12] even within the microcanonical ensemble as we will discuss later. It should be noticed that the partitions which fall in the energy region corresponding to the canonical temperature jump are hardly sampled by the canonical ensemble, but are accessible in the microcanonical ensemble. Therefore, in a finite system the microcanonical sorting of events allows to study regions of the phase diagram which are forbidden in the canonical formalism. These regions are characterized by specific properties such as negative

heat capacities which we will later on study in more detail. In particular it is important to identify experimental observables which can directly inform us about these peculiar properties.

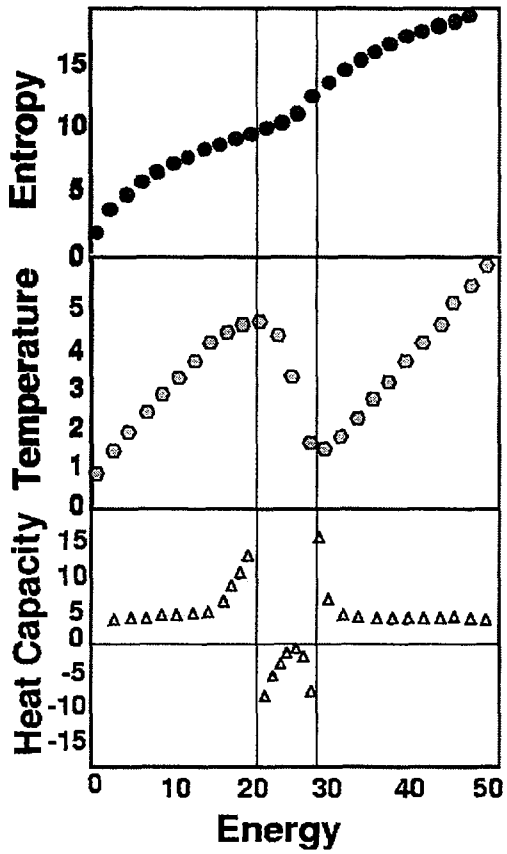

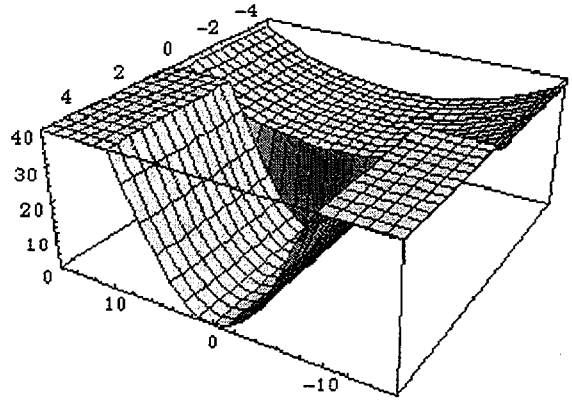

$$H=e_1(N_1-A_1^2+A^2)+e_2N_2$$

Figure 5. Right part: schematic drawing of the double quantum oscillator model with the associated hamiltonien. Left part: the entropy, temperature and heat capacity as a function of the excitation energy.

3.2. Analytical quantum models

In the lattice-gas model the connection between a phase transition and a back bending in the caloric curve appears evident. However, one may worry about the generality of such a statement. Is it a general property found in many systems? Do such anomalies also exist in quantum systems or is this definition of phase transition restricted to classical systems? In order to address this question we have investigated a model of A particles which can jump from one harmonic oscillator to an other. In the first one all particles strongly interact while in the second one they are free. The curvature of the second well plays the role of a confining potential i. e. of a pressure. The corresponding Hamiltonian reads

$$\hat{\mathbf{H}} = \varepsilon_1 \left(\hat{\mathbf{N}}_1 - \hat{\mathbf{A}}_1^2 + A^2\right) + \varepsilon_2 \hat{\mathbf{N}}_1 \tag{9}$$

with the operators

$$\hat{\mathbf{N}}_i = \sum_{n=1}^{A} \delta_{in}^{i} a_n^{+} a_n \tag{10}$$

$$\hat{\mathbf{A}}_i = \sum_{n=1}^{A} \delta^i_{i_n} \tag{11}$$

where i_n is the harmonic well occupied by the particle i. Using this Hamiltonian we can compute the level density and so the entropy. To simplified the calculation we have chosen ε_1 and ε_2 to be commensurable.. Then, we can compute the temperature and the associated heat capacity (see figure 5). We observe that the system indeed presents an anomaly in the curvature of the entropy. Back-bending and negative heat capacities automatically follow.

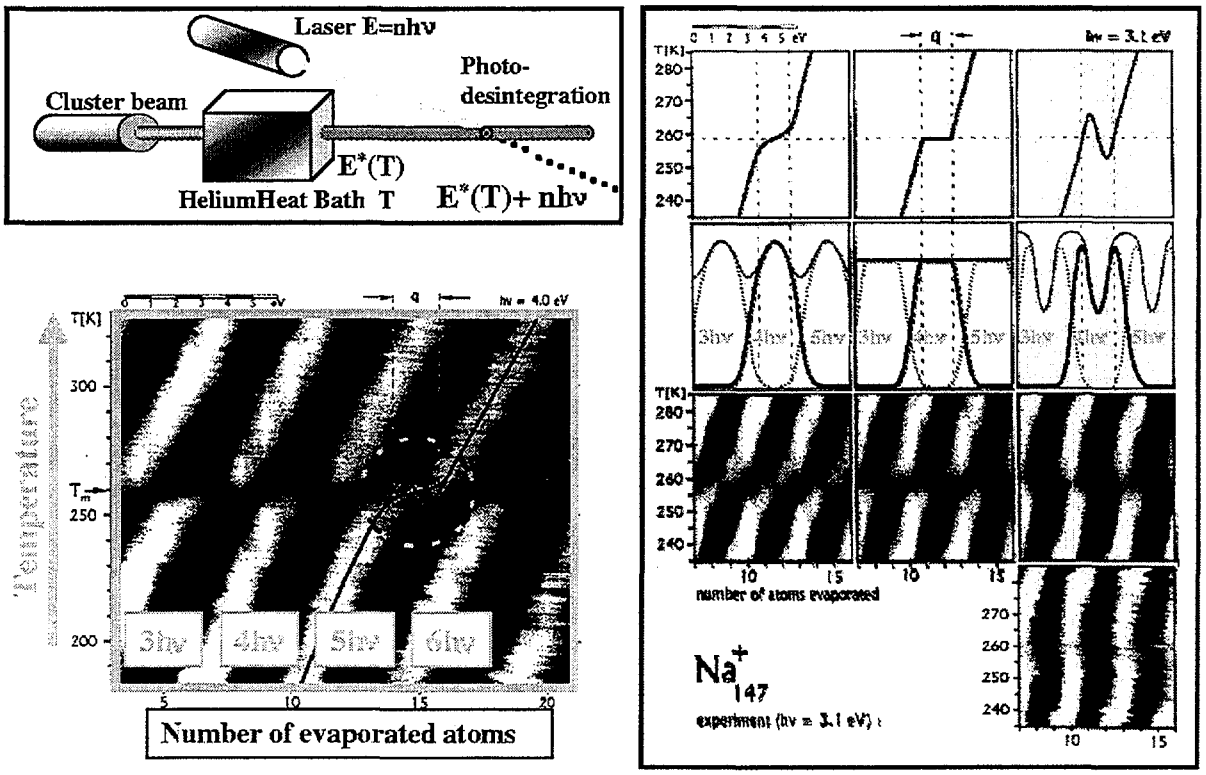

Figure 6. Left top part: a schematic picture of the experimental set-up. Below: the observed correlation between the temperature of the oven and the fragmentation pattern induced by the absorption of several photons. On the right several scenarii for the transition between two phases are compared with the experimental results. The observed pattern is only compatible with the existence of a back-bending[13].

4. EXPERIMENTAL SIGNALS.

4.1. Melting of clusters [13]

In the year 2000 the first experimental signature of a back bending caloric curve has been reported in the melting of metallic clusters. The experiment is rather simple. The clusters are first produced and selected. Then the clusters get thermalized in the melting region in an helium heat bath. After thermalization they are further excited by a laser beam absorbing several photons, thanks to the plasmon vibration (see figure 6). The energy is then such that the cluster has time to evaporate atoms within the experiment time scale. The number of evaporated atoms provides a measure of the cluster energy

distribution. Changing the temperature the thermal excitation changes and the distribution of evaporated atoms is shifted. The obtained bidimensional pictures of the number of evaporated atoms as a function of the oven temperature clearly show an anomaly corresponding to the melting point. If now we consider a back bending or a monotonous caloric curve the energy distribution goes from a bi-modal to a mono-modal shape. This induces a modification of the fragmentation pattern. The observed pattern is only compatible with a negative heat capacity system.

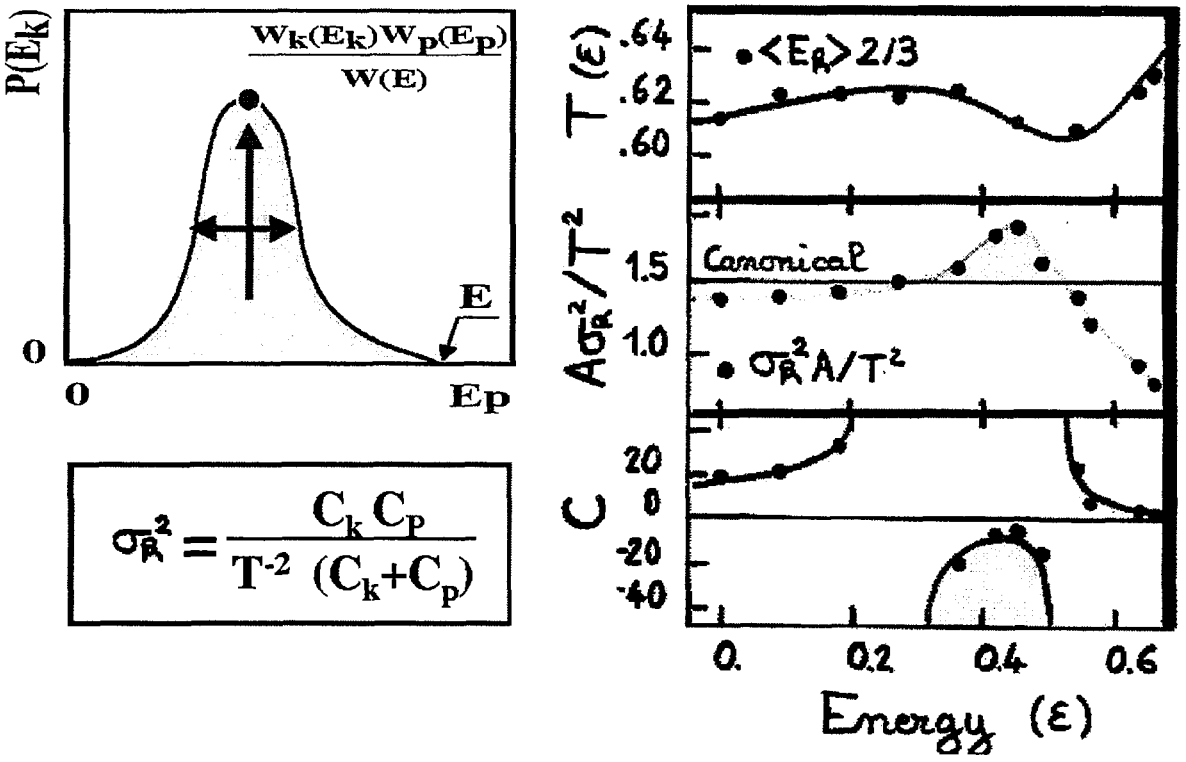

Figure 7. Left part: the schematic distribution of partial energy for a fixed total energy. Right: the comparison of the various measurements (dots) with the exact results of the lattice-gas model (lines).

4.2. Negative heat capacities and abnormal fluctuations

Recently many progresses have been performed in order to extract the nuclear thermodynamics from experimental data. Vaporization threshold have been measured by the INDRA collaboration[14]. Among the most famous attempts stands the ALADIN caloric curve which shows a saturation in the temperature (plateau) in the phase transition region [15]. More recently the possibility to signal this transition using the fluctuation of the energy partition has been investigated [11,16,17] and the presence of a negative heat capacity have been reported [18,19].

The investigation method can be easly explained for a classical fluid and tested in the framework of the lattice-gas model. The total energy E (here including the external constraining potential field) of the considered system can be decomposed into two independent components, its kinetic and potential energy: $E = E_k + E_p$. In a microcanonical ensemble with a total energy E the total degeneracy factor $W(E) = \exp(S(E))$ is thus simply given by the folding product of the individual degeneracy factors $W_i(E_i) = \exp(S_i(E_i))$

of the two subsystems $i = k, p$. One can then define for the total system as well as for the two subsystems the microcanonical temperatures T_i and the associated heat capacities C_i. Since we are dealing with a classical gas the kinetic equation of state is simply given by $E_k = 3AT_k/2$ and the kinetic heat capacity is a constant, $C_k = 3A/2$. If we now look at the kinetic energy distribution when the total energy is E we get

$$P_k^E(E_k) = \exp\left(S_k(E_k) + S_p(E - E_k) - S(E)\right) \tag{12}$$

Using Eq.(12) we directly get that the most probable partitioning of the total energy E between the potential and kinetic components is characterized by a unique microcanonical temperature $\bar{T} \equiv T_k\left(\bar{E}_k^E\right) = T_p\left(E - \bar{E}_k^E\right)$. Therefore the most probable kinetic energy $\bar{E}_k^E$ can be used as a microcanonical thermometer as shown in Figure 7. Using a Gaussian approximation for $P_k^E(E_k)$ the kinetic energy variance can be calculated as [20]

$$\sigma_k^2 = \bar{T}^2 \frac{C_k C_p}{C_k + C_p} \tag{13}$$

where C_k and C_p are the microcanonical heat capacities calculated for the most probable energy partition.

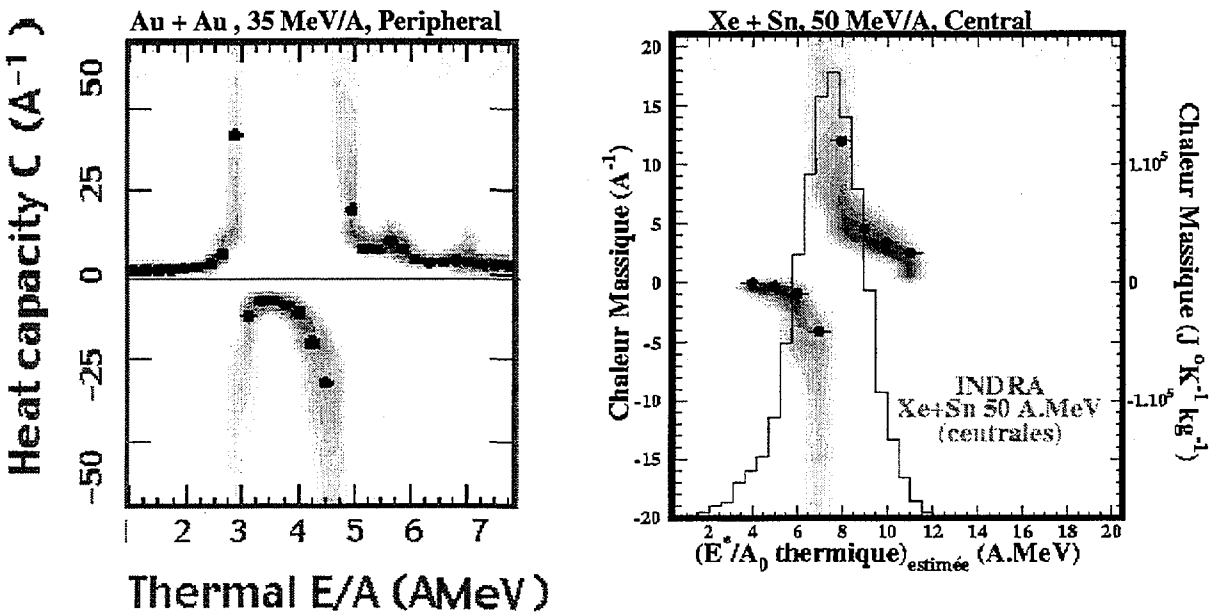

Figure 8. Several microcanonical heat capacity extracted from the kinetic energy fluctuations by the MULTICS collaboration (left) and the INDRA one).

As shown in Figure 7 when C_p diverges and then becomes negative, σ_k^2 remains positive but overcomes the canonical expectation $\sigma_k^2 = \bar{T}^2 C_k$. This anomalously large kinetic energy fluctuation is a signature of the first order phase transition. Equation (13) can be inverted to extract from the observed fluctuations the heat capacity

$$C \simeq C_k + C_p = \frac{\bar{T}^2 C_k^2}{\bar{T}^2 C_k - \sigma_k^2} \tag{14}$$

Figure 7 shows that the heat capacity extracted from the kinetic energy fluctuations is in very good agreement with the exact one. This means that kinetic energy fluctuations are an experimentally accessible measure of the heat capacity which allows to sign divergences and negative branches characteristic of the phase transition.

Examples of experimental use of the proposed signal of the phase transition are given in figure 8. The important point to notice is that now the study of the nuclear phase transition is becoming quantitative.

5. ROLE OF THE VOLUME.

As far as the liquid-gas phase transition is concerned it is essential to discussed the role of the volume since it is the order parameter and since we know that the divergency of the heat capacity depends upon the isobar or isochore character of the considered transformation.

5.1. Caloric curves and abnormal fluctuations

The normalized fluctuations $\sigma_K^2/{T_\lambda}^2$ obtained in the microcanonical ensemble with a constrained average volume, $< V >_\lambda$, are shown in the energy-λ plane in figure 9 together with the isotherms. One can clearly see that up to the critical temperature the fluctuations are abnormally large in the coexistence region. From figures 9 it is apparent that the phase transition signal is visible in the temperature as well as in the fluctuation observable.

However the experimentally measured caloric curves are not bidimensional. Indeed, even if different sources with different excitation energies can be prepared, the other thermodynamical parameters are not controlled even if they can be measured. In particular an average value for the freeze-out volume of a selected ensemble of events can be deduced from interferometry and correlation measurements or through comparisons with statistical models but it cannot be varied independently of the deposited energy. This means that experiments are sampling a monodimensional curve on the equation of state surface. The resulting caloric curve therefore depends on the actual transformation in the thermodynamical parameters plane. As an example the behavior of the temperature as a function of energy at a constant pressure or a constant average volume in the subcritical region is displayed in the upper part of figure 9. At constant pressure the caloric curves are steeper than the ones at constant λ when the system is in the liquid or in the vapor phase; in the coexistence region the isobars are almost identical to the iso-λ's since P_λ and λ differ only by the temperature which is almost constant in the phase transition region, and a back-bending is clearly seen. On the other hand at constant average volume a smooth behavior is observed with a slope change entering the gas phase, as expected from general thermodynamics (see also [8,12]) . This is due to the fact that the λ parameter varies rapidly in the coexistence region. From these examples one clearly sees that the various transformations lead to very different caloric curves. More generally, it is clear that the back-bending of the temperature surface can be avoided depending on the path of the considered transformation and the phase transition signal can be hidden in the observation of the caloric curve.

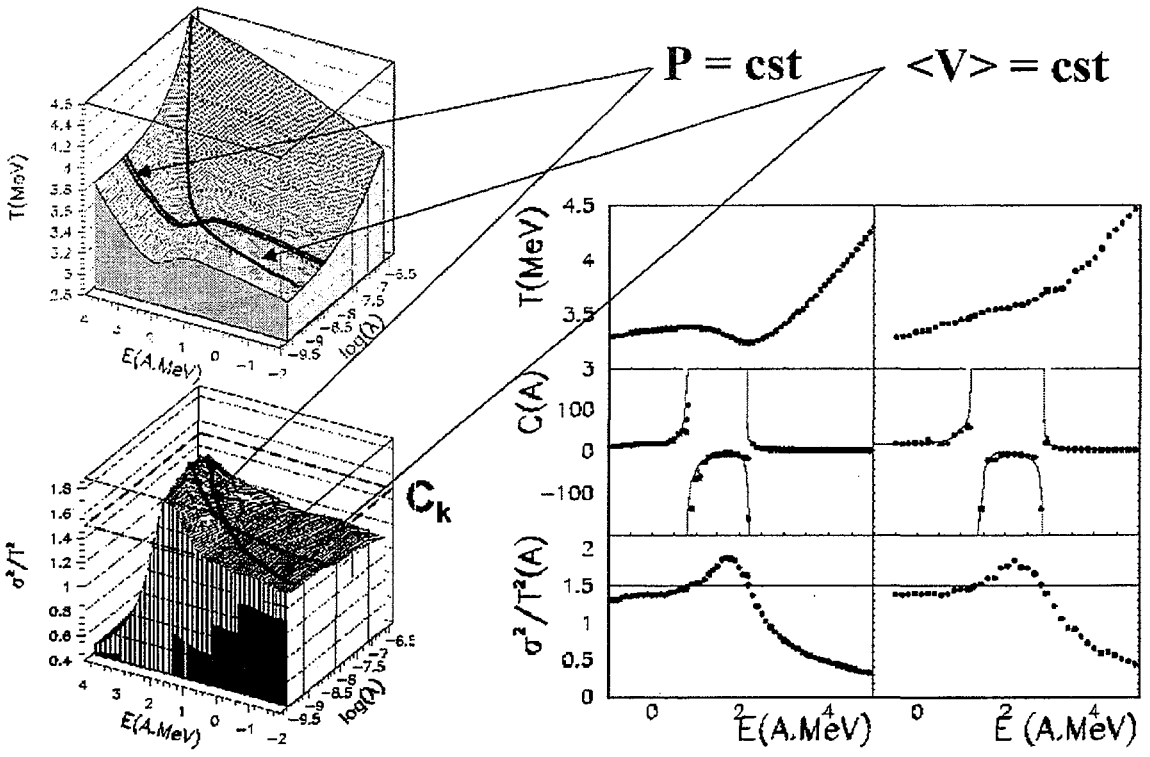

Figure 9. Left part : Isotherms and contour plot of the normalized kinetic energy fluctuations in the Lagrange parameter versus energy plane. The level corresponding to the canonical expectation $\sigma_1^2/T^2 = 1.5$ is shown. Thick line: critical isotherm. Right pannel : Thermodynamical quantities in the microcanonical ensemble for a transformation at constant pressure and at constant volume (right part). Upper panels: caloric curve. Lower panels: normalized kinetic energy fluctuations compared to the canonical expectation (lines). Medium panels: heat capacity (symbols) compared to the estimation through eq.(14) (lines) at constant pressure (left part) and at constant volume (right part).

On the other side partial energy fluctuations are a state variable which does not depend on the transformation from one state to another and can directly give access to the equation of state. From figure 9 we can see that in the whole phase transition region the microcanonical fluctuations present a strong maximum which exceeds the canonical value: an anomalously large fluctuation signal will be always seen if the system undergoes a first order phase transition, independent of the path. As an example the lower part of figure 9 shows a constant P_λ or $< V >_\lambda$ cut of the bidimensional fluctuation surface. The quantitative behavior of the heat capacity as a function of energy depends on the specific transformation, but at each point the heat capacity extracted from fluctuations is a direct measure of the underlying equation of state. This is clearly demonstrated in the medium part of figure 9 which compares the exact heat capacity C_λ with the fluctuation approximation. The agreement between the two results illustrates the accuracy of the estimation (14).

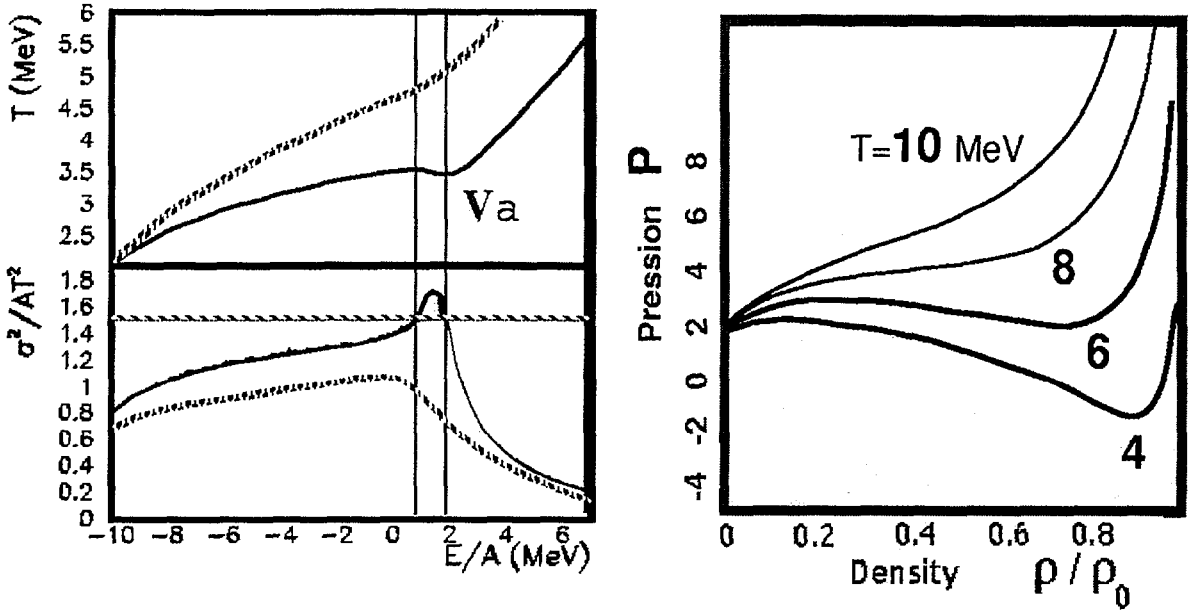

Figure 10. Left part the caloric curve and associated fluctuations in a constant volume ensemble at two different values of the the box volum (higer for the solid line) [21]. The anomalous fluctuations are always linked with the presence of a back bending in the caloric curve. Right: isotherms of a canonical ensemble at constant volume in the pressure versus density plane[22]. The EOS clearly exhibit anomalies associated with negative compressibilities.

5.2. Constant volume transformation and negative compressibility

We now turn to the constant volume ensembles i.e. ensembles defined through the presence of sharp boundary conditions. As expected, for small boxes, this ensemble does not presents anomalies in the equation of states. Indeed, the heat capacity at constant volume is not expected to diverge in the thermodynamical limit. Only the infinite volume solution which can also be thought as a zero pressure system presents the back bending already discussed in the context of open systems. (see figure 10). The absence of a back bending in the caloric curve does not mean that the phase transition is not present. Indeed, varying the volume one can see that the thermodynamical potential has a convexity anomaly. In such a case the compressibility is negative. This clearly shows that the volume is the order parameter therefore controlling the order parameter allows to explore the phase transition region and to spot the back bending characteristic of first order phase transition in the associated conjugated variable, here the pressure. This is illustrated in the case of the canonical ensemble at constant volume in the right part of figure 10. One can clearly see that the isotherms present a strong back bending below the critical temperature. It should be noticed that this demonstrates that the existence of back-bending's is not limited to the microcanonical ensemble. In fact the best ensemble to spot a first order phase transition is the one in which the order parameter is directly constrained. Then a back bending should be seen in the associated EOS i.e. the equation giving the conjugated variable (the second derivative of the thermodynamical potential) as a function of the order parameter no matter the variables chosen to control the other

thermodynamical degrees of freedom. Conversely, if the order parameter is controlled only in average its conjugated variable appears as a Lagrange multiplier controlling the statistical ensemble. Then the order parameter EOS does not back-bends any more since only one average order parameter is allowed for a given Lagrange multiplier. However, if another intensive variable is controlled and happens to be different in the two phases (for example here the energy) then it may play the role of an alternative order parameter and the associated EOS (here the caloric curve) may present an anomaly.

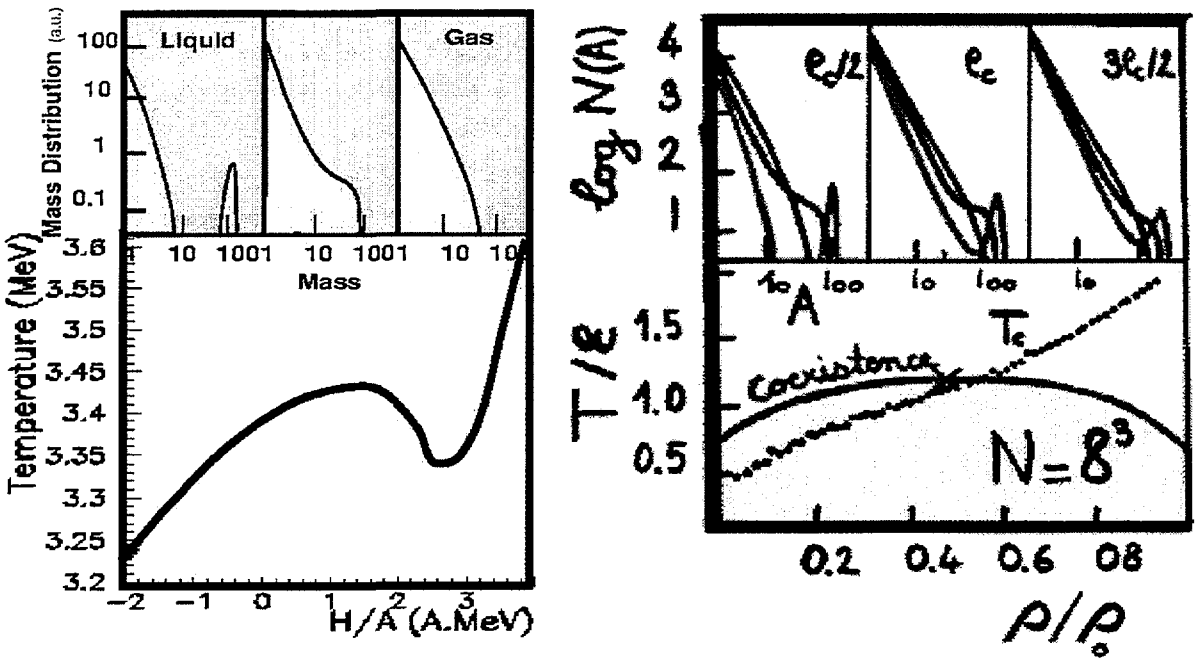

Figure 11. Left part : microcanonical fragment size distribution at three different energies presented on top of the associated caloric curve. Right part: canonical fragment distribution for three density regions. Subcritical, critical and supercritical distributions are shown. The corresponding critical temperature for each density are reported in the phase diagram below.

6. ADDITIONAL SIGNALS OF A PHASE TRANSITION.

6.1. Critical mass partitions

In order to better characterize the back-bending region it is interesting to examine the properties of the associated partitions. It should be noticed that since the back bending region of a microcanonical calculation corresponds to events with a very small probability in a canonical ensemble one may expect that the microcanonical sampling can be different from the typical partitions of the corresponding canonical distribution. Figure 11 presents canonical and microcanonical fragment mass distributions in the phase transition region[11]. Let us first start with the microcanonical ensemble, at the lowest energy, in the first uprising branch of the caloric curve, the fragment distribution shows an exponential fall off of light fragments associated with the gas phase and a big liquid drop, characteristic of a subcritical system. At the highest energy corresponding to the beginning of

the gas branch of the caloric curve, the distribution resembles to a typical supercritical vaporized system. In the middle of the back-bending region a critical distribution is observed. This observation of a critical behavior of the fragment size distribution in the coexistence region has also been reported in the canonical lattice-gas context [4] (shown in the figure 11). Critical behaviors are observed irrespectively of the considered density. Therefore, a line of critical points can be identified in the whole phase diagram, from a percolation type at high density toward the thermodynamical critical point and down to the interior of the coexistence region. The microcanonical study additionally suggests that anomalous fluctuations coming from the negative heat capacity characteristic of a microcanonical first order phase transition, are to be expected in the region where the fragment size distribution becomes critical. The conjunction of these two observations signs of a first order phase transition.

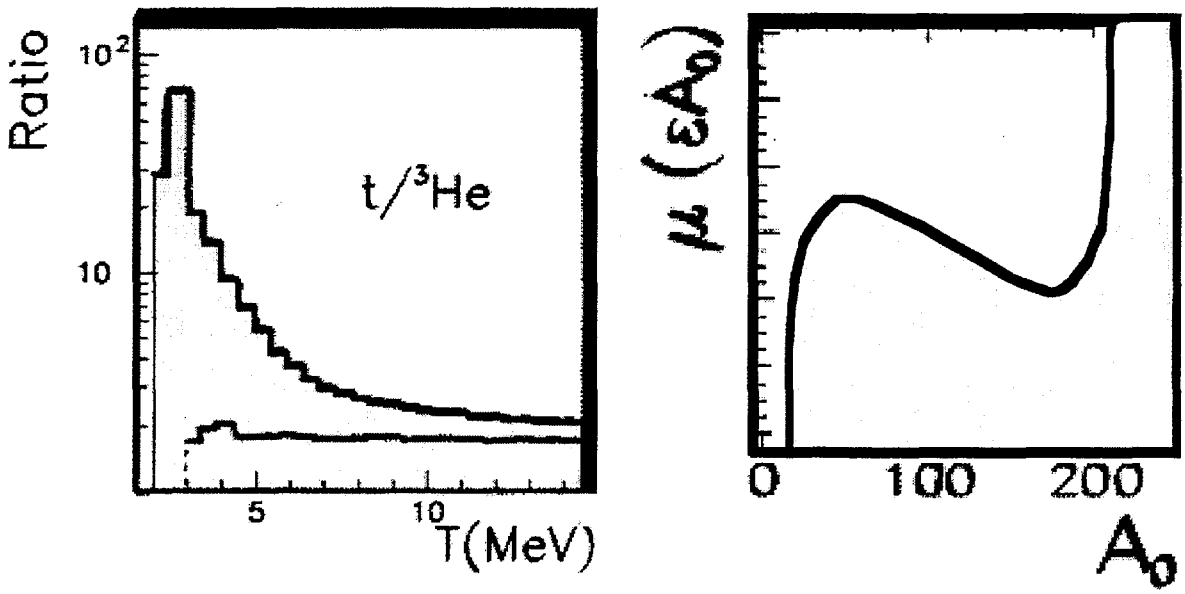

Figure 12. Left part: t/He isotopic ratio calculated for an asymetric matter at various temperature (full line) compared to the combinatorial expectation (thin line); right part: the evolution of the canonical chemical potential as a function of the number of particles.

6.2. Chemical signals

Since we are dealing with a liquid gas phase transition in a two fluid system one also expects the presence of a distillation (or fractionation) of the isospin asymmetric nuclear matter. This was stressed first in ref. [23] and then illustrated in isospin dependent lattice-gas model [7]. This result showing a strong neutron enrichment of the gas phase (light fragments) is reported in figure 12. This may provide an additional signal of the phase transition. Finally we would like to stress that a back-bending should also be expected in the chemical potential curve as a function of the number of constituents. A reflection about chemical fluctuation in presence of a negative curvature of the thermodynamical potentials when the number of constituents is modified should also be considered. Indeed, one may think that if two parts of the system exchange particles the anomalous curvature will lead to anomalously large fluctuations. This should be further studied but may help

to spot first order phase transition in many situations where it is also associated with chemical equilibria.

7. Conclusions

Phase transitions are universal properties of matter in interaction. They have been widely studied in the thermodynamical limit of infinite systems. However, in many physical situations this limit cannot be accessed and so phase transitions should be reconsidered from a more general point of view. This is for example the case of matter under long range forces like gravitation. Even if these self gravitating systems are very large they cannot be considered as infinite because of the non saturating nature of the force. Other cases are provided by microscopic or mesoscopic systems *built out of matter which is known to present phase transitions.* Metallic clusters can melt before being vaporized. Quantum fluid may undergo Bose condensation or super-fluid phase transition. Dense hadronic matter should merge in a quark and gluon plasma phase while nuclei are expected to exhibit a liquid -gas phase transition. For all these systems the theoretical and experimental issue is how to sign a possible phase transition in a finite system.

In this contribution we have shown that convexity anomalies of the thermodynamical potentials can be used to signal and to define phase transitions. We have presented the first experimental evidences of such a phenomenon. We have discussed in details the role of the volume in the liquid-gas phase transitions and explained why caloric curves are not unique since they depend upon the volume of the system at the various considered energies. Conversely we have stressed that fluctuations are state properties which can be used to infer the thermodynamics of the considered ensemble of events. Finally we have stress that the fragmentation patterns as well as the chemical properties can be used as complementary information to control the existence of a phase transition.

REFERENCES

1. A. Guarnera, PhD thesis GANIL Caen (1996).
2. D.H.E. Gross, Phys. Rep. 279 (1997) 119.
3. D.H.E Gross et al., cond-mat/9911257
4. F.Gulminelli and P.Chomaz, Phys. Rev. Lett. 82 (1999) 1402.
5. C.N. Yang and T.D. Lee, Phys.Rev. 87 (1952) 410.
6. J.M.Carmona et al., Nucl. Phys. A 643 (1998) 115
7. P.Chomaz and F.Gulminelli, Phys. Lett. B447 (1999) 221.
8. X. Campi and H. Krivine, Nucl. Phys. A 620 (1997) 46 and Physica A, in press.
9. J. Pan and S. Das Gupta, Phys.Rev. C 51 (1995) 1384; Phys.Rev.Lett. 80 (1998)1182.
10. V.Duflot et al., Phys.Lett.B, in press.
11. F.Gulminelli et al., Europhys.Lett., 50 (2000)434
12. J.M.Carmona et al., nucl-th/9910061 and J.Borg et al., Phys.Lett. B 470 (1999) 13.
13. M. Schmidt et al, Nature 393 (1998) 238 and to be published
14. M. F. Rivet et al., Phys. Lett. B 388 (1996) 219; B. Borderie et al.,Phys. Lett. B 388 (1996) 224.
15. J. Pochodzalla et al., Phys.Rev.Lett. 75 (1995) 1040; Y. G. Ma et al, Phys.Lett. B 390 (1997) 41.

16. P.Chomaz and F.Gulminelli, Nucl. Phys. A647, 153 (1999).
17. P.Chomaz, F.Gulminelli and V. Duflot, Phys. Rev. Lett. in press (2000).
18. M. D'Agostino et al., Nucl.Phys. A 650 (1999) 329 and Phys.Lett.B 473 (2000) 219.
19. R. Bougault et al, cont. to the XXXVIII Winter meeting on nucl. Phys. Bormio (Italy), Ed. I. Iori
20. J.L.Lebowitz et al., Phys.Rev. 153 (1967) 250.
21. F. Gulminelli et al, cont. to the XXXVIII Winter meeting on nucl. Phys. Bormio (Italy), Ed. I. Iori
22. H.Mueller and B.D. Serot, Phys.Rev. C 52 (1995) 2072.